



Correlations of Multi-component Ground Motions in Eastern Canada

Najib Bouaanani¹, Ilona Bartosh²

¹ Professor, Dept. of Civil, Geological and Mining Engineering, Polytechnique Montréal - Montréal, QC, Canada.

² Ph.D. Student, Dept. of Civil, Geological and Mining Engineering, Polytechnique Montréal - Montréal, QC, Canada.

ABSTRACT

This paper presents an investigation of inter-component correlations of seven earthquakes recorded in eastern Canada between 1982 and 2010, namely Miramichi (1982), Nahanni (1985), Saguenay (1988), Cap Rouge (1997), La Malbaie (1997), Rivière-du-Loup (2005), and Val-des-Bois (2010). The three-component accelerograms recorded at each site are uncorrelated to obtain and characterize principal axes, corresponding Arias intensity ratios and vertical inclination angles. Mean horizontal and vertical intensity ratios and standard deviations are given and their values discussed as a function of soil type and epicentral distance. Characterizations of peak ground accelerations and period-dependent spectral amplifications along the principal directions are also carried out to assess the impact on the response of engineering structures. Particular attention is devoted to evaluate the relationship between horizontal principal acceleration components and the geometric mean of recorded horizontal accelerations, a measure commonly used to define horizontal spectral demands in ground motion prediction equations and code-prescribed design or uniform hazard spectra. The implications of the obtained results on the selection of appropriate multi-directional seismic input for structures in eastern Canada are illustrated. The intensity- and spectral-based characterizations presented provide an improved understanding and assessment of multi-directional seismic input in Eastern Canada, but the methodology proposed can be easily applied to other regions.

Keywords: 3D ground motions; Earthquake principal components; Arias intensity; Multi-component seismic input; Eastern North America Seismicity.

INTRODUCTION

Assessing the seismic behavior and design of structures is of utmost importance to ensure safe and reliable infrastructure in earthquake prone areas. Along with catastrophic damage caused by recent earthquakes worldwide, significant progress has been made in understanding complex strong ground motion mechanisms and seismic design and analysis procedures have been continuously improved to take into account new seismological findings and experimental evidence. Earthquake events are commonly characterized by three translational acceleration components measured along the three orthogonal axes of an array of seismographs. Rotational acceleration components are not directly measured and are generally neglected. In structural engineering, it is usual practice to carry out seismic analyses using only one horizontal acceleration component or one horizontal and one vertical acceleration components (or two horizontal components). The dynamic response of most structures is however intrinsically three-dimensional (3D), and the combined effects of multi-component accelerations may be required for critical structures such as bridges, dams, nuclear power plants, as well as asymmetric structures (Menun and Der Kiureghian, 2000; Lopez et al., 2000; Ghersi and Rossi, 2001; Menun, 2004; Radeva et al., 2005; Rigato and Medina, 2007; Crestel and Bouaanani, 2007; Fujita and Takewaki, 2010). Indeed, a thorough assessment of the seismic response requires that earthquake loading be applied along directions that produce the most critical effects. Critical loading cases depend on the structure's geometrical and mechanical properties, as well as on the incident angles of the impinging seismic waves. Thanks to recent developments in numerical and software techniques, 3D seismic analyses are being increasingly used in everyday structural engineering projects. Modern seismic codes recommend different approaches with varying degrees of sophistication, including modal response spectrum methods, and linear or non-linear time-history analyses. In this regard, selecting the appropriate seismic input is a key factor in the structural analysis of critical infrastructure. Previous research on ground motions from different regions has shown that recorded earthquake components are generally statistically cross-correlated (Penzien and Watabe, 1975; Kubo and Penzien, 1976; Loh et al., 1982; Radeva et al., 2005; López et al., 2006). To allow for a rigorous comparison between different incident angles, earthquake components used for the analysis have to be uncorrelated statistically. Several codes and guidelines such as IAEA (2003), CSA (2010a), CSA (2010b), ICOLD (2010) and NIST (2011) specify that multi-directional seismic analyses should be conducted using statistically uncorrelated ground motion components. In moderate seismicity regions, simulated

ground motions are usually used to compensate for the scarcity of recorded earthquakes. The characteristics of the synthetic ground motions must then account properly for inter-component correlations (Kubo and Penzien, 1979; Yeh and Wen, 1989; Heredia-Zavoni and Machicao-Barrionuevo, 2004; Rezaeian and Der Kiureghian, 2012). Studies of these correlations have been conducted for earthquakes which occurred in various regions such as California, Japan, the Pacific Ring of Fire and Mexico (Penzien and Watabe, 1975; Kubo and Penzien, 1976; Loh et al., 1982; López et al., 2006; Hong and Goda, 2010). Similar studies were rarely reported for ground motions recorded in eastern North America and relevant information is therefore lacking to select appropriate multi-component seismic input for 3D seismic analyses in this region. This paper aims at studying inter-component correlations of seven earthquakes recorded in eastern Canada between 1982 and 2010. The recorded ground motions are uncorrelated and the resulting components characterized in terms of intensity and spectral ratios. A particular attention is also devoted to evaluate the relationship between horizontal principal acceleration components and the geometric mean of recorded horizontal accelerations, a measure commonly used to define horizontal spectral demands in ground motion prediction equations (GMPEs) and code-prescribed design or uniform hazard spectra (UHS).

DATABASE OF HISTORICAL UNCORRELATED GROUND MOTIONS

Selected recorded ground motions

The ground motions investigated in this work were recorded during the Miramichi (1982), Nahanni (1985), Saguenay (1988), Cap Rouge (1997), La Malbaie (1997), Rivière-du-Loup (2005), and Val-des-Bois (2010) earthquakes. These seven events caused only minor property damage, but they have provided a wealth of information to characterize ground motions in ENA's particular intra-plate environment. Although the Nahanni earthquakes occurred in northwest Canada, they are included herein since their ground motions were found appropriate for seismic analysis of critical facilities in ENA (Wetmiller et al., 1988, Atkinson and Boore, 1998). For each event, ground accelerations a_X , a_Y and a_Z recorded at different sites along instrument horizontal axes X and Y , and vertical axis Z , respectively, are studied. The records were obtained from different sources (LDEO 2007, GSC 2011, Atkinson 2011).

Uncorrelated ground motions

The accelerations recorded along the three orthogonal components of an earthquake are naturally correlated, considering that they result from the same ground motion source and same seismic waves traveling through the same medium from source to site. The correlations between the three ground motion components recorded at each station can be investigated by examining the individual contributions of each component to the total energy released during the shaking. For this purpose, the methodology proposed by Penzien and Watabe (1975) is applied herein. We first determine the matrix $\boldsymbol{\mu}$ of covariances μ_{ij} of the three translational time history accelerations $a_i(t)$, $i = X, Y, Z$, at a given site as

$$\mu_{ij} = \frac{1}{t_f - t_i} \int_{t_i}^{t_f} a_i(t) a_j(t) dt \quad i, j = X, Y, Z \quad (1)$$

in which t_i and t_f denote the first and last times of the interval of interest of the shaking duration, respectively. Applying a technique similar to finding the principal axes of a stress tensor in a solid body, a coordinate system in which the matrix $\boldsymbol{\mu}$ is diagonal can be obtained. These principal axes define directions along which earthquake signals are statistically uncorrelated. The resulting principal variances μ_1 , μ_2 and μ_3 are ordered as major, intermediate and minor, respectively: $\mu_1 \geq \mu_2 \geq \mu_3$. The maximum, intermediate and minor principal axes correspond to directions along which maximum, intermediate and minor earthquake energy is released, respectively.

CHARACTERIZATION OF GROUND MOTION COMPONENTS IN TERMS OF INTENSITY RATIOS

Definition of intensity ratios and vertical inclination angle

The eigenvectors corresponding to the principal variances are identified to distinguish the *most* vertical of the three principal axes, i.e. the eigenvector making the smallest angle with the geographical vertical axis Z at a given site. This axis is denoted V and the corresponding principal covariance μ_V . We designate by θ_V the vertical inclination angle between the geographical vertical axis Z at the recording site and the *most* vertical principal axis V as illustrated in Fig. 1. This angle may vary between 0° and 90° , taking a value of 0° when axes V and Z coincide. The two other horizontal principal variances are denoted μ_{H_1} and μ_{H_2} , and are referred to as major and minor horizontal variances, respectively, with $\mu_{H_1} \geq \mu_{H_2}$. The corresponding eigenvectors identify the major and minor horizontal principal axes, denoted 1 and 2, respectively, as indicated in Fig. 1. The angle between the projection $1'$ of the major horizontal principal axis and the epicentral direction relating the site to the epicenter is denoted as θ_H . This angle varies between 0° and 180° , and is positive clockwise. Its value is 0° when the principal axis points to the epicenter. The epicentral angle θ_E defines the direction from each site to the epicenter. This angle is evaluated with respect to the North, is positive clockwise and may vary between 0° and 360° .

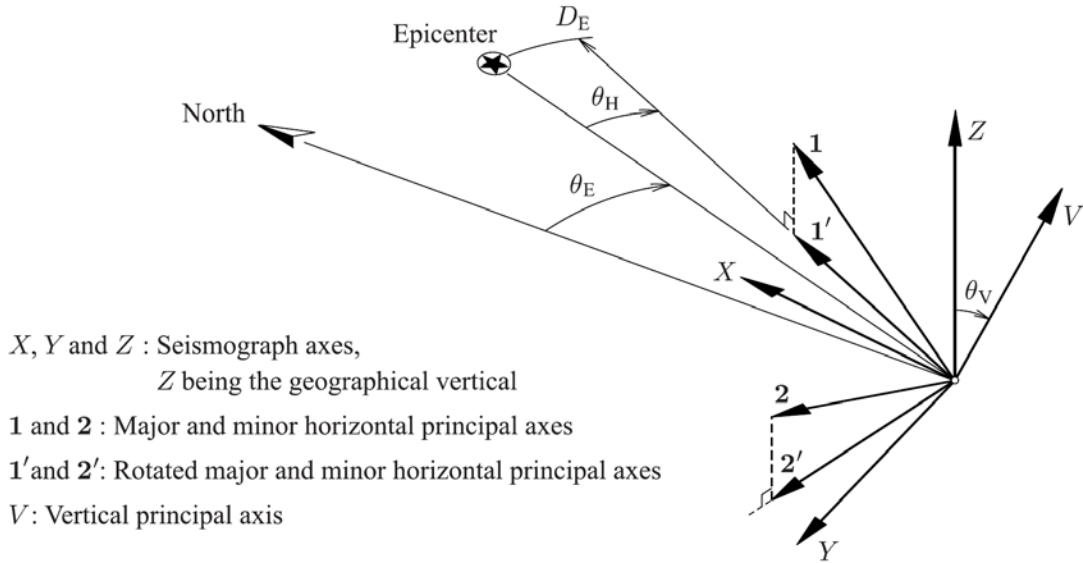


Figure 1. Definitions of principal axes and angles.

The following covariance ratios can then be defined $\gamma_H = \mu_{H_2}/\mu_{H_1}$ and $\gamma_V = \mu_V/\mu_{H_1}$. We note that the ordering of the calculated vertical and horizontal variances cannot be predicted. Any of the three following cases could then be expected

$$\mu_{H_1} \geq \mu_{H_2} \geq \mu_V; \quad \mu_{H_1} \geq \mu_V \geq \mu_{H_2}; \quad \mu_V \geq \mu_{H_1} \geq \mu_{H_2} \quad (2)$$

The order of the covariances for a given ground motion is important since it informs on the relative significance of the three principal directions in terms of Arias intensity.

It is particularly interesting to identify whether the vertical principal direction corresponds to the minor, intermediate or major intensity. It is also useful to interpret the horizontal intensity ratio γ_H as a measure of the relative importance of the intensities of the two horizontal principal components, and the vertical intensity ratio γ_V as an indication of the relative importance of the intensity along the vertical direction.

Results

Following the technique outlined in the previous section, the principal axes and corresponding intensity ratios defined in Section 3.1 are determined by averaging over the entire duration of each accelerogram. The variations of intensity ratios as a function of epicentral distance are illustrated in Fig. 2. Mean values of 0.60 and 0.50 are obtained for γ_H and γ_V , respectively, considering all ground motions and soil types. The standard deviations corresponding to γ_H are lower than those corresponding to γ_V . Practically the same mean values and standard deviations are obtained when only rock sites are considered. A mean γ_H value of 0.55 is found for soil sites, which is of the same order of magnitude as the mean value obtained for all sites. The mean γ_V value, i.e. 0.36, corresponding to soil sites is lower than that corresponding to all sites. However, the smaller size of the database corresponding to soil sites prevents from any firm generalization of this trend. The mean vertical inclination angles θ_V vary from 16.67° for soil sites (Standard deviation of 10.66°) to 20.34° for rock sites (Standard deviation of 13.05°). These values are higher than the total average vertical deviation of 11.4° (Standard deviation of 9.9°) found by López et al. (2006) for earthquakes from the Pacific Ring of Fire, and 11.3° (Standard deviation of 10°) reported by Hong and Goda for intraplate California records. Finally, Fig. 2 shows linear trends for data from rock sites. The slightly increasing trend for γ_H suggests that the energy contents of horizontal principal components become closer with larger epicentral distance, while the slightly decreasing trend for γ_V suggests that the energy content of the vertical principal component vanishes with respect to that of the major horizontal component as epicentral distance expands. The results of this section characterized uncorrelated ground motions in terms of intensity ratios, which represent ratios of seismic energy inputs at recording sites along principal directions. Characterization of peak ground accelerations and spectral amplifications along these directions is also required to assess the impact on the response of engineering structures. Such characterization is presented in the next section.

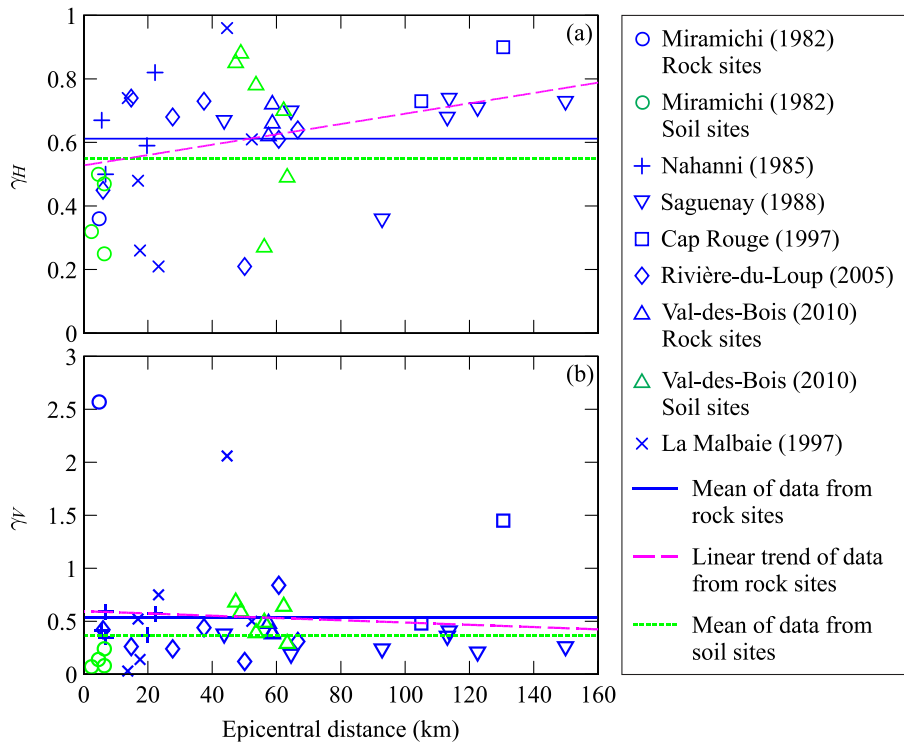


Figure 2. Variation of horizontal and vertical intensity ratios as a function of epicentral distance: (a) γ_H and (b) γ_V .

SPECTRAL RATIOS OF GROUND MOTION HORIZONTAL COMPONENTS

Definition of spectral ratios

A basic evaluation of the relative amplitudes of the two horizontal components of a ground motion is first carried-out by introducing the ratio $\rho_0 = a_{H_2}^*/a_{H_1}^*$, where $a_{H_1}^*$ and $a_{H_2}^*$ denote the PGAs of the horizontal principal components H_1 and H_2 , respectively. This ratio is however independent of structural response. To include the effects of structural period variations, the 5% -damped acceleration response spectra of the previously described ground motions are computed. The relationship between maximum horizontal spectral acceleration response amplitudes can then be characterized using the ratio $r_A = A_{H_2}^*/A_{H_1}^*$, with $A_{H_1}^*$ and $A_{H_2}^*$ denoting the maximum spectral accelerations of principal components H_1 and H_2 , respectively. It is also important to track the relative importance of horizontal spectral acceleration amplitudes as a function of period T . For this purpose, we define the ratio $\rho(T) = A_{H_2}(T)/A_{H_1}(T)$, where $A_{H_1}(T)$ and $A_{H_2}(T)$ denote the spectral accelerations of principal components H_1 and H_2 at period T , respectively. This ratio measures the similarity of two horizontal components in terms of frequency content, i.e. the two components are more similar as the ratio is closer to 1. The geometric mean is commonly used to define horizontal acceleration spectral demands in GMPEs (Boore et al., 2006; Campbell and Bozorgnia, 2007). It is therefore important to evaluate the relationship between this measure and horizontal principal components which define minor and major acceleration demands in terms of Arias intensity. Such investigation can be conducted for a given set of ground motions by developing new GMPEs along principal directions and comparing the results to those based on the geometric mean of horizontal components (Hong and Goda, 2007; Hong and Goda, 2010). In the present work, we introduce an alternative methodology based on the direct statistical evaluation of the following spectral ratios defined at each period T as $\bar{\rho}_1(T) = A_{H_1}(T)/\sqrt{A_X(T)A_Y(T)}$ and $\bar{\rho}_2(T) = A_{H_2}(T)/\sqrt{A_X(T)A_Y(T)}$, where A_X and A_Y are the acceleration spectra corresponding to recorded accelerograms a_X and a_Y , respectively. The ratios $\bar{\rho}_1$ and $\bar{\rho}_2$ measure the closeness, in terms of spectral amplitude and frequency content, of major and minor horizontal acceleration components, respectively, to the geometric mean of the recorded horizontal acceleration components.

Results

The ratios defined in the previous section are computed for acceleration components uncorrelated considering Trifunac-Brady duration as it was shown to provide stable results. Figure 3 illustrates the variation of ratios ρ_0 and r_A as a function of epicentral distance. It can be seen that: (i) PGA ratio ρ_0 varies from 0.26 (respectively 0.40) to 1.10 (resp. 1.07), with a mean value of

0.67 (resp. 0.65) for rock (resp. soil) sites; (ii) spectral amplitude ratio r_A varies from 0.22 (respectively 0.37) to 1.16 (resp. 0.91), with a mean value of 0.70 (resp. 0.59) for rock (resp. soil) sites. It is important to note that both ratios are generally lower than one, except at: (i) one rock and two soil sites for ρ_0 , and (ii) three rock sites for r_A . This result means that the major horizontal principal components H_1 of the ground motions studied are generally associated with maximum horizontal PGAs and maximum horizontal spectral accelerations. The similarity between mean values of ratios ρ_0 and r_A suggests that the energy-based relative importance of horizontal components is not significantly affected by structural response amplifications. Practically the same increasing linear trends are obtained for ratios ρ_0 and r_A considering data from rock sites. Such increasing trends suggest that the spectral amplitudes of horizontal principal components become closer with larger epicentral distance. Variations of frequency-dependent spectral ratios ρ , $\bar{\rho}_1$ and $\bar{\rho}_2$ are studied next over a period range from 0 to 10s. This wide period range is considered for comprehensive identification of global trends, although spectral ratios at very long periods should be interpreted with care because of the generally vanishing spectral accelerations at these periods as well as possible long-period noise due to analog-to-digital conversions. The obtained results are shown in Fig. 4 for rock and soil sites. We emphasize however that results for soil sites are given here only for comparison purposes and that no conclusive trends should be deduced from the related comments below as they are based on a small amount of available soil data.

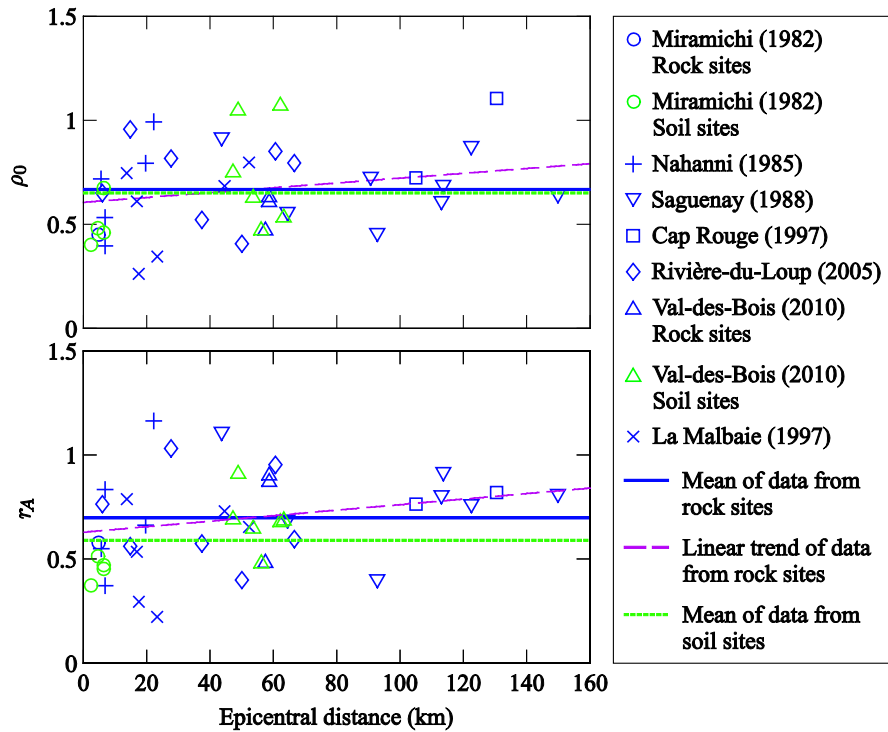


Figure 3. Variation of ratios ρ_0 and r_A as a function of epicentral distance: (a) ρ_0 ; (b) r_A .

It can be seen from Fig. 4 (a) that the mean value of spectral ratio ρ for rock sites varies from around 0.7 at short periods to around 0.9 at longer periods. More scatter around the mean value is however observed at the longer period range as illustrated by the individual curves. Figs. 4 (b) and (c) present the variations of spectral ratios $\bar{\rho}_1$ and $\bar{\rho}_2$ on rock sites, respectively. These results reveal that: (i) the mean spectral ratio $\bar{\rho}_1$ is greater than 1, varying from around 1.27 at short periods to around 1.20 at longer periods, and (ii) the mean spectral ratio $\bar{\rho}_2$ is lower than one, varying from around 0.80 at short periods to around 0.90 at longer periods. Figs. 4 (d), (e), and (f) present variations of spectral ratios ρ , $\bar{\rho}_1$ and $\bar{\rho}_2$ for soil sites and contain more pronounced fluctuations due to the smaller amount of data available on soil sites. The order of magnitude of the mean values at the short and long period ranges is approximately the same as rock sites. Finally, the spectral ratios ρ , $\bar{\rho}_1$ and $\bar{\rho}_2$ are evaluated as a function of period ranges that characterize the response of typical structures, from very stiff to very flexible. The following period ranges are considered: $[0s - 0.1s]$; $[0.1s - 0.4s]$; $[0.4s - 0.6s]$; $[0.6s - 1s]$; $[1s - 2s]$; $[2s - 4s]$; $[4s - 6s]$ and $[6s - 10s]$. The spectral ratios obtained for rock sites according to these period ranges are illustrated in Fig. 5. In this figure, the eight stacks of bars represent the eight period intervals described previously. Each bar corresponds to a pair of two horizontal acceleration components at each site, organized by ascending epicentral distances, the shortest being at the left of each stack of bars. This graphical representation first shows that there is no clear trend related to the effect of epicentral distance on spectral ratios. It also illustrates that the scatter of results increases for higher periods, while mean values are practically stable for the whole range of periods. These observations are confirmed by Table 9 giving the mean values and standard deviations corresponding to ratios ρ , $\bar{\rho}_1$ and $\bar{\rho}_2$ as a function of period range.

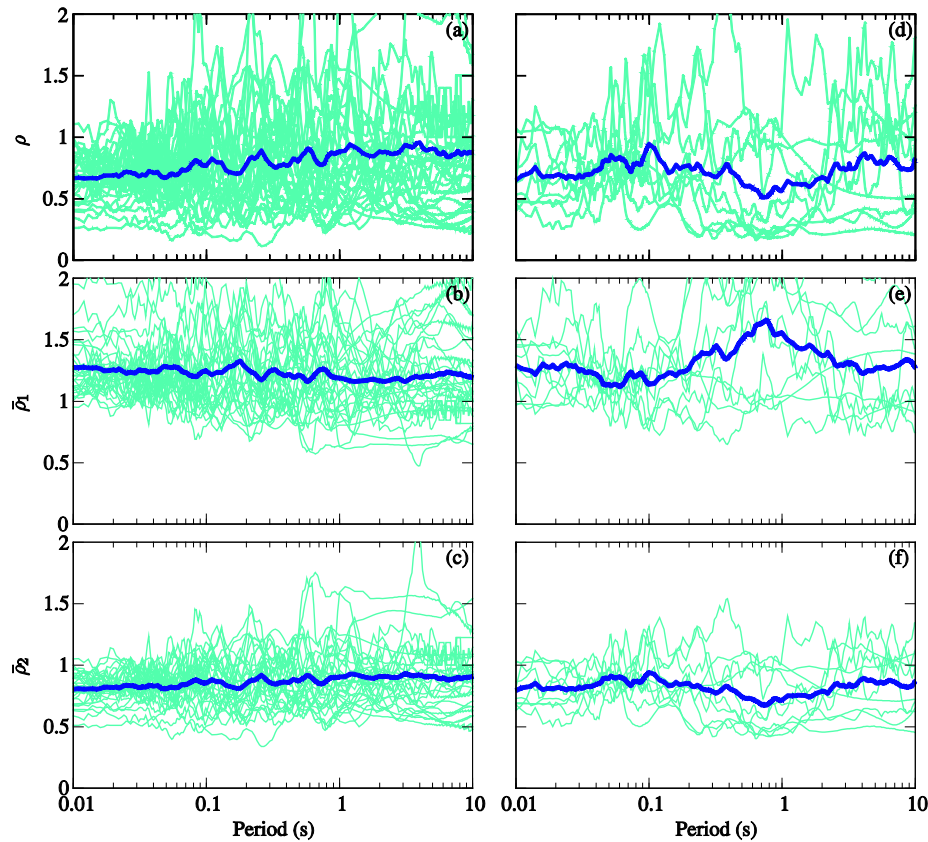


Figure 4. Variation of spectral ratios ρ , $\bar{\rho}_1$ and $\bar{\rho}_2$ as a function of period: (a) to (c) Rock sites; (d) to (f) Soil sites.

CONCLUDING REMARKS

This paper presented an investigation of inter-component correlations of seven earthquakes recorded in eastern Canada between 1982 and 2010, namely Miramichi (1982), Nahanni (1985), Saguenay (1988), Cap Rouge (1997), La Malbaie (1997), Rivière-du-Loup (2005), and Val-des-Bois (2010). The three-component accelerograms recorded at each site were uncorrelated to obtain and characterize principal axes, corresponding Arias intensity ratios and vertical inclination angles. We first showed that using the Trifunac-Brady duration yields stable results when compared to the entire earthquake duration. We also found a strong correlation between the vertical component and the minor principal intensity, a trend that was observed for earthquakes recorded in other regions of the world. Mean intensity ratios and standard deviations were given and their values discussed as a function of soil type and epicentral distance. Characterizations of peak ground accelerations and period-dependent spectral amplifications along the principal directions were also carried out to assess the impact on the response of engineering structures. We found that the major horizontal principal components of the ground motions studied are generally associated with maximum horizontal PGAs and maximum horizontal spectral accelerations. We also evaluated the relationship between horizontal principal components and the geometric mean of recorded horizontal accelerations, a measure commonly used to define horizontal spectral demands in GMPEs and code-prescribed design or uniform hazard spectra. For practical purposes, the spectral ratios were given as a function of different period ranges that characterize the response of typical structures, from very stiff to very flexible. The results presented above can be used as key indicators to help in selecting appropriate multi-component input accelerograms for 3D time-history analyses and evaluating two-component spectral acceleration demands for bi-directional dynamic modal response analyses.

ACKNOWLEDGEMENTS

The authors would like to acknowledge the financial support of the Natural Sciences and Engineering Research Council of Canada (NSERC) and les Fonds de recherche du Québec en nature et technologies (FRQNT).

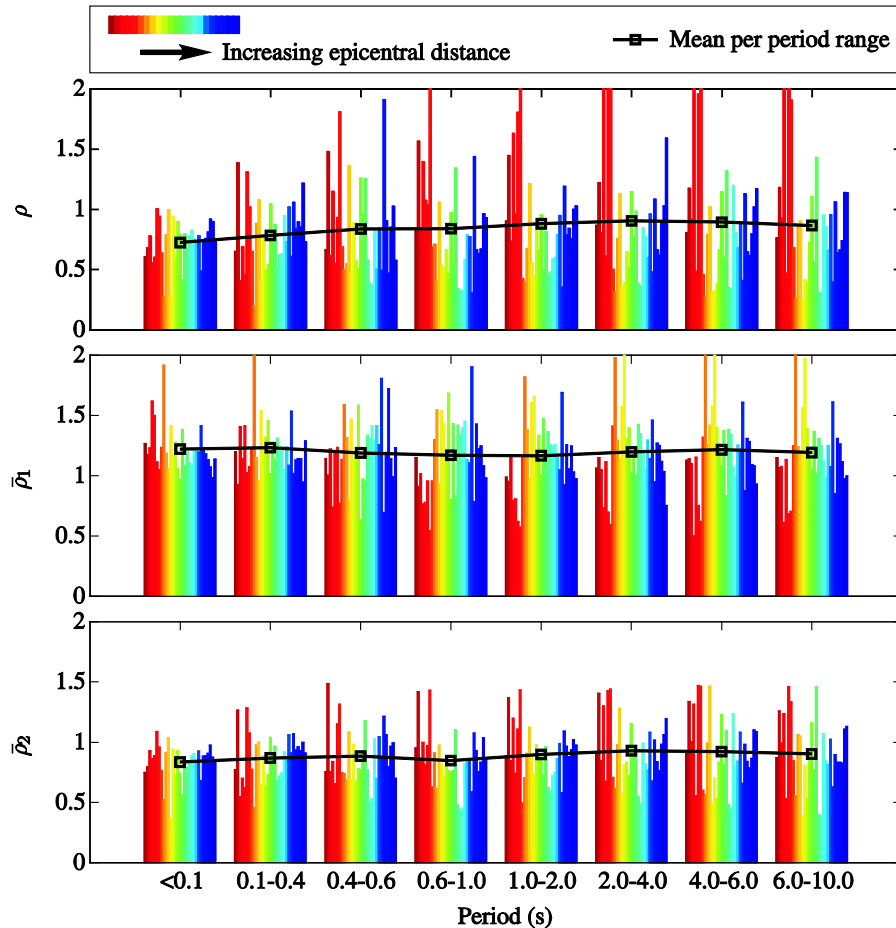


Figure 5. Variation of spectral ratios ρ , $\bar{\rho}_1$ and $\bar{\rho}_2$ of uncorrelated ground motions as a function of period ranges: (a) Spectral ratio ρ ; (b) Spectral ratio $\bar{\rho}_1$; and (c) Spectral ratio $\bar{\rho}_2$.

REFERENCES

- [1] Arias A (1970), "A measure of earthquake intensity," RJ Hansen, editor, *Seismic Design for Nuclear Power Plants*, pp. 438–483, MIT Press, Cambridge, Massachusetts.
- [2] Atkinson GM (2011), "Engineering Seismology Toolbox," Available from: <http://www.seismotoolbox.ca>, Date accessed: 30 July 2011.
- [3] Bent AL (2009), "A Moment Magnitude Catalog for the 150 Largest Eastern Canadian Earthquakes," *Geological Survey of Canada*, Open File 6080.
- [4] Boore DM, Watson-Lamprey J, Abrahamson NA (2006), "Orientation-independent measures of ground motion," *Bull Seismol Soc Am*, 96(4A): 1502-1511.
- [5] Campbell KW and Bozorgnia Y (2007), "Campbell-Bozorgnia NGA ground motion relations for the geometric mean horizontal component of peak and spectral ground motion parameters," Report No. PEER-2007/02, Pacific Earthquake Engineering Research Center, University of California, Berkeley.
- [6] Canadian Standards Association (CSA) (2010a), "Ground motion determination for seismic qualification of nuclear power plants," N289.2-10, Mississauga, Ontario, Canada.
- [7] Canadian Standards Association (CSA) (2010b), "Design procedures for seismic qualification of nuclear power plants," N289.3-10, Mississauga, Ontario, Canada.
- [8] Crestel B and Bouaanani N (2007), "Earthquake response of short to medium span cable-stayed bridges," *9th Canadian Conference on Earthquake Engineering*, Ottawa, Canada.
- [9] Fujita K and Takewaki I (2010), "Critical correlation of bi-directional horizontal ground motions," *Eng Struct*, 32: 261-272.

- [10] Geological Survey of Canada (GSC), Earthquakes Canada, "Strong Motion Data Sets," <http://earthquakescanada.nrcan.gc.ca>, Date accessed: 27 September 2011.
- [11] Ghersi A and Rossi PP (2001), "Influence of bi-directional ground motions on the inelastic response of one-storey in-plan irregular systems," *Eng Struct*, 23: 579–591.
- [12] Heredia-Zavoni E and Machicao-Barrionuevo R (2004), "Response to orthogonal components of ground motion and assessment of percentage combination rules," *Earthquake Eng Struct Dynam*, 33:271–284.
- [13] Hong HP and Goda K (2007), "Orientation-dependent ground-motion measure for seismic-hazard assessment," *Bull Seismol Soc Am*, 97: 1525–1538.
- [14] Hong HP and Goda K (2010), "Characteristics of horizontal ground motion measures along principal directions," *Earthq Eng & Eng Vib*, 9: 9–22.
- [15] International Atomic Energy Agency (IAEA) (2003), "Seismic design and qualification for nuclear power plants," *Safety guide*, No. NS-G-1.6, Vienna, Austria.
- [16] International Commission on Large Dams (ICOLD) (2010), "Selecting seismic parameters for large dams - Guidelines", Revision of Bulletin 72.
- [17] Kubo T and Penzien J (1976), "Time and frequency domain analysis of three dimensional ground motions San Fernando earthquakes," Report no. EERC 76-6, College of Engineering – University of California, Berkeley, California, 232 p.
- [18] Kubo T and Penzien J (1979), "Simulation of three-dimensional strong ground motions along principal axes, San Fernando earthquake," *Earthquake Eng Struct Dynam*, 7:279–294.
- [19] Lamont-Doherty Earth Observatory (LDO), Earthquake Strong Motion Database, National Center for Earthquake Engineering Research (LDEO/NCEER), <http://www.ldeo.columbia.edu>, Date accessed: 10 October 2007.
- [20] Loh CH, Penzien J, and Tsai YB (1982), "Engineering analyses of smart 1 array accelerograms," *Earthquake Eng Struct Dynam*, 10(4): 575–591.
- [21] López OA, Chopra AK and Hernandez JJ (2000), "Critical response of structures to multicomponent earthquake excitation," *Earthquake Eng Struct Dynam*, 29: 1759–1778.
- [22] López OA, Hernandez JJ, and Bonilla R (2006), "Response spectra for multicomponent structural analysis," *Earthquake Spectra*, 22(1): 85–113.
- [23] Macias-Carrasco M, Fereydouni A, Goda K, and Atkinson GM (2010), "Documentation for the Canadian Composite Seismicity Catalogue (CCSC09)," Available from: <http://www.seismotoolbox.ca/Documents/CCSC09.pdf>, Date accessed: 15 December 2012.
- [24] Menun C and Der Kiureghian A (2000), "Envelopes for seismic response vectors. II: Application," *J Struct Eng*, 126(4): 474–481.
- [25] Menun C (2004), "An envelope for Mohr's circle in seismically excited three-dimensional structures," *Earthquake Eng Struct Dynam*, 33: 981–998.
- [26] National Research Council of Canada (NRCC) (2010), "National Building Code of Canada," Ottawa, Ont.
- [27] National Institute of Standards and Technology (NIST) (2011), "Selecting and scaling earthquake ground motions for performing response-history analyses," *NEHRP Consultants Joint Venture*, NIST GCR 11-917-15.
- [28] Penzien J and Watabe M (1975), "Characteristics of 3-dimensional earthquake ground motions," *Earthquake Eng Struct Dynam*, 3(4): 365–374.
- [29] Radeva ST, Scherer RJ, and Radev D (2005), "Strong motion waves estimation for seismic control of nuclear power plants," *Nucl Eng Des*, 235(17-19): 1977-1988.
- [30] Rezaeian S and Der Kiureghian A (2012), "Simulation of orthogonal horizontal ground motion components for specified earthquake and site characteristics," *Earthquake Eng Struct Dynam*, 41(2): 335-353.
- [31] Rigato AB and Medina RA (2007), "Influence of angle of incidence on seismic demands for inelastic single-storey structures subjected to bi-directional ground motions," *Eng Struct*, 29: 2593–2601.
- [32] Trifunac MD and Brady AG (1975), "A study on the duration of strong earthquake ground motion," *Bull Seismol Soc Am*, 65(3): 581–626.
- [33] United States Geological Survey (USGS) (2012), "Earthquake Search USGS/NEIC (PDE) 1973 - 2012 11 30 Database," <http://earthquake.usgs.gov/earthquakes/eqarchives/epic/>, Date accessed: 01 December 2012.
- [34] Wetmiller RJ, Horner RB, Hasegawa HS, North RG, Lamontagne M, Weichert DH, and Evans SG (1988), "An analysis of the 1985 Nahanni earthquakes," *Bull Seism Soc Am*, 78: 590-616.
- [35] Yeh CH and Wen YK (1989), "Modeling of nonstationary earthquake ground motion and biaxial and torsional response of inelastic structures," *Civil Engineering Studies*, Structural Research Series Report No. 546, University of Illinois.